Aluminium doped $Zn_{1-x}Mg_xO$ – a transparent conducting oxide with tunable optical and electrical properties

K. Fleischer,[1, a)] E. Arca,[1] C. Smith,[1] and I.V. Shvets[1]
Cleaner Energy Laboratory and CRANN, School of Physics, Trinity College Dublin, Dublin 2, Ireland

(Dated: 30 August 2012)

A ternary mixed oxide $Zn_{1-x}Mg_xO$ has been doped with aluminium to create a range of transparent conducting oxides (TCOs) with tunable refractive index as well as work function. Conductive material was synthesised up to a magnesium concentration of x=0.45, although the conductivity is reduced compared to standard ZnO:Al. The changes in band gap, work function and conductivity have been attributed to a modified band structure and energetic position of the aluminium induced donor state.

Transparent conducting oxides are an important class of material for various optoelectronical devices such as liquid crystal displays (LCDs), organic light emitting diodes, and thin film solar cells.[1–4] One particularly important material is aluminated zinc oxide (AZO, ZnO:Al). It offers good conductivity and high transparency in the visible range for lower costs than the commonly used indium tin oxide (ITO). One drawback of any of the known TCOs based on ITO or doped binary oxides such as ZnO:Al and SnO_2:F is the limited flexibility in regards to refractive index and work function. Greater flexibility in tuning the refractive index of a TCO would reduce unwanted reflections at internal interfaces, if such modified TCOs are employed as internal anti-reflective layers.[5] Greater flexibility in the work function could help in reducing serial resistances at TCO-active layer interfaces caused by unfavourable band alignment.

A ternary system, where tunablility in band gap and refractive index has already been demonstrated is the system of hexagonal $Zn_{1-x}Mg_xO$. Magnesium can be incorporated at zinc positions up to high values of $x \sim 0.5$ while maintaining the hexagonal crystal structure of the zinc oxide.[6–8] Incorporation at higher values of x remains difficult due to the instability of the hexagonal phase of MgO. Indeed the tunability of the optical properties has already been employed in ZnO based LEDs, where either the emission energy can be tuned or the material can be used as wave guide for the optically denser ZnO active emitter in multi quantum well structures.[7,9–11]

It has been shown further that the flexibility in work function using such a ternary system can be used to improve CIGS solar cell efficiencies. Such a material with selected work function can be deployed as a buffer layer between a conventional ZnO:Al front electrode and the p-type chalcogenide absorber.[12] The improvement demonstrated by Törndahl et.al.[12] was small, as the conductivity of the $Zn_{1-x}Mg_xO$ layers used decreased substantially compared to n-type ZnO commonly used. This increases serial resistance within the buffer layer even if the interfacial serial resistance is reduced. To compensate for this an effective doping of the buffer layer itself is required.

[a)] Electronic mail: fleisck@tcd.ie

Previous studies have shown that $Zn_{1-x}Mg_xO$ up to x=0.3 can be doped with Al, though not as efficiently as plain ZnO.[13–15] Compared to ZnO:Al a significant reduction in conductivity was observed and related to a decrease in carrier concentration and electron mobility in the disordered lattice.[13,14] Within this study the system was further investigated and electrical properties were correlated to optical and crystal structure properties, as well as composition analysis with XPS. We confirmed the changes in conductivity, though they have been attributed to changes in mobility *and* carrier activation energy.

Samples were grown by spray pyrolysis on microscope glass slides (Fisher brand) using methanol as a solvent and organic precursor salts. Zinc acetate dihydrate ($Zn(CH_3CO_2)_2 \cdot 2H_2O$), magnesium acetate tetrahydrate ($Mg(CH_3CO_2)_2 \cdot 4H_2O$) and aluminum acetyl acetonate ($Al(C_5H_7O_2)_3$, AAA) have been used as Zn, Mg, and Al precursors respectively.

Crystal properties were measured by XRD (Bruker D8 Advance). Optical properties have been determined by UV-VIS Spectrophotometry (Varian Cary 50) and variable angle spectroscopic ellipsometry (Sopra GESP 5). Electrical measurements have been performed in van-der-Pauw 4 point probe configuration, chemical composition by X-ray photo electron spectroscopy (XPS) and work function as well as valence band structure by UPS (Omicron Multiprobe XP). As growth rates vary upon introduction of large quantities of the Mg precursor, the thickness of each sample has been determined independently by cross sectional SEM (Zeiss Ultra) on cleaved samples. This minimises the error in the determination of the resistivity, carrier concentration and improves the ellipsometric analysis.

All samples show a columnar growth, with (0001) oriented crystals (see Fig. 1). Films are highly texturised with a preferential crystal orientation. The SEM top view image (inset Fig. 1) clearly shows the hexagonal, columnar structure. A compression of the c-axis with increased Mg content is observed by the systematic shift of the (002) reflex to higher angles. For samples with a Mg content of x=0.37 dephasing occurred, and (100) oriented MgO planes are detected as well. Based on the development of the MgO content as measured by XRD

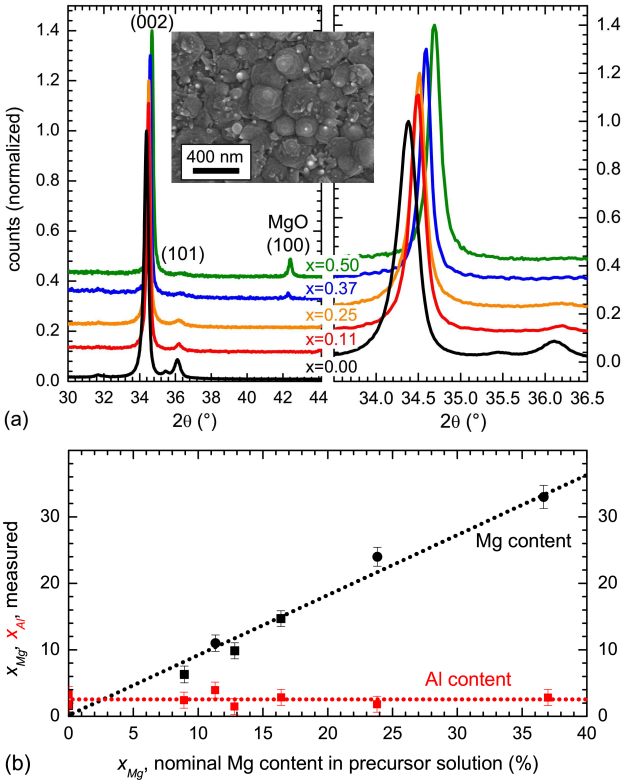

FIG. 1. (a) X-Ray diffraction patterns of $Zn_{1-x}Mg_xO$:Al for various magnesium content (x). (b) Confirmation of the incorporated amount of Mg and Al measured by XPS.

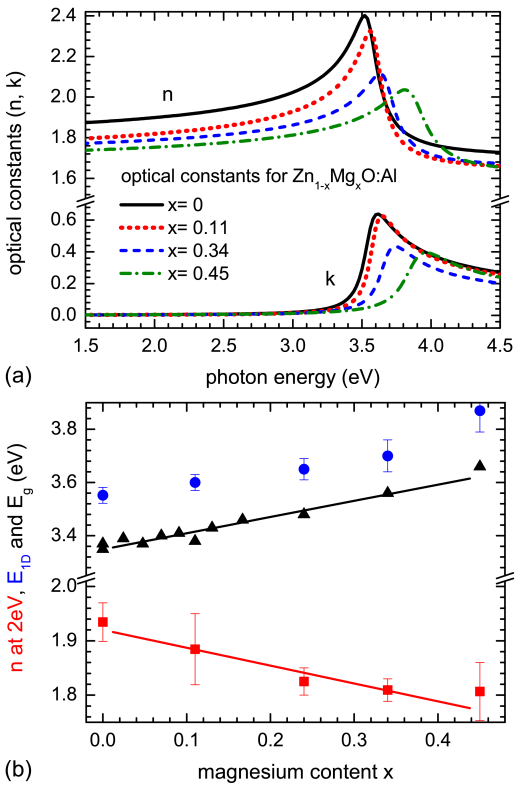

FIG. 2. (a) Model dielectric function fitted to measured multiple angle ellipsometric measurements. The change in the band gap position is clearly seen, as well as the reduction of the refractive index in the transparent region. (b) Dependency of the refractive index n at 2eV (■), 1D oscillator position E_{1D} (●), and band gap E_g (▲) on Mg content.

for x<0.3 pure phases of $Zn_{1-x}Mg_xO$:Al can be grown by spray pyrolysis. XPS studies reveal a similar Mg content in the $Zn_{1-x}Mg_xO$:Al films as the nominal concentration within the precursor solution. The incorporated Al content was also not affected by the presence of Mg (Fig. 1b).

Figure 2 shows the results of the optical analysis of the samples. The samples show the expected opening of the band gap and reduction of the refractive index n in line with previous results for undoped $Zn_{1-x}Mg_xO$.[7,8]. The ZnO dielectric function was fitted with a single 1D bulk critical point[16], as this method not only describes the shape of the refractive index in the transparent region, but also accurately models the onset of absorption and the position of a maximum k. For comparison the optical band gap E_g as determined by the onset of absorption in UV-VIS transmission measurements (Tauc-plot) is also shown. The energetic position of the 1D bulk critical point is systematically higher, but follows the same trend. Please note that our spray pyrolysis grown samples do not show carrier concentrations high enough to observe additional band gap openings due the Burstein-Moss effect unlike the one observed in studies using pulsed laser deposition or magnetron sputtering.[13–15] The significant reduction in n for high Mg concentration makes the material interesting for internal anti-reflective layers.[5]

Figure 3 shows the summary of the main electrical properties investigated. Foremost a decrease in work function with increasing Mg content has been noted by the shift in the secondary electron cut off in UPS measurements, which is related to the work function.[17] For this analysis only samples with low resistivity of $\rho < 0.1\Omega$cm have been analysed to avoid systematic errors due to charging.

The resistivity ρ increases with increasing Mg content, while the refractive index as well as work function decrease. However even at a Mg content of 0.33 a residual conductivity of >0.5 Scm^{-1} remains, making the material useful as modified TCO. It was previously reported, that the increase in ρ is solely related to the decrease in mobility and reduction of carrier concentration. The latter could be caused by a decreased incorporation of Al in the mixed $Zn_{1-x}Mg_xO$ lattice or changes in the dopant energy level and an identification of the particular mechanism was not feasible so far.[13,15] As our analysis clearly shows, the Al content, within the error of the measurement, is not affected by the large quantities of Mg in the lattice (Fig. 1b). However changes in the carrier activation energy E_a, as determined by an Arrhenius plot

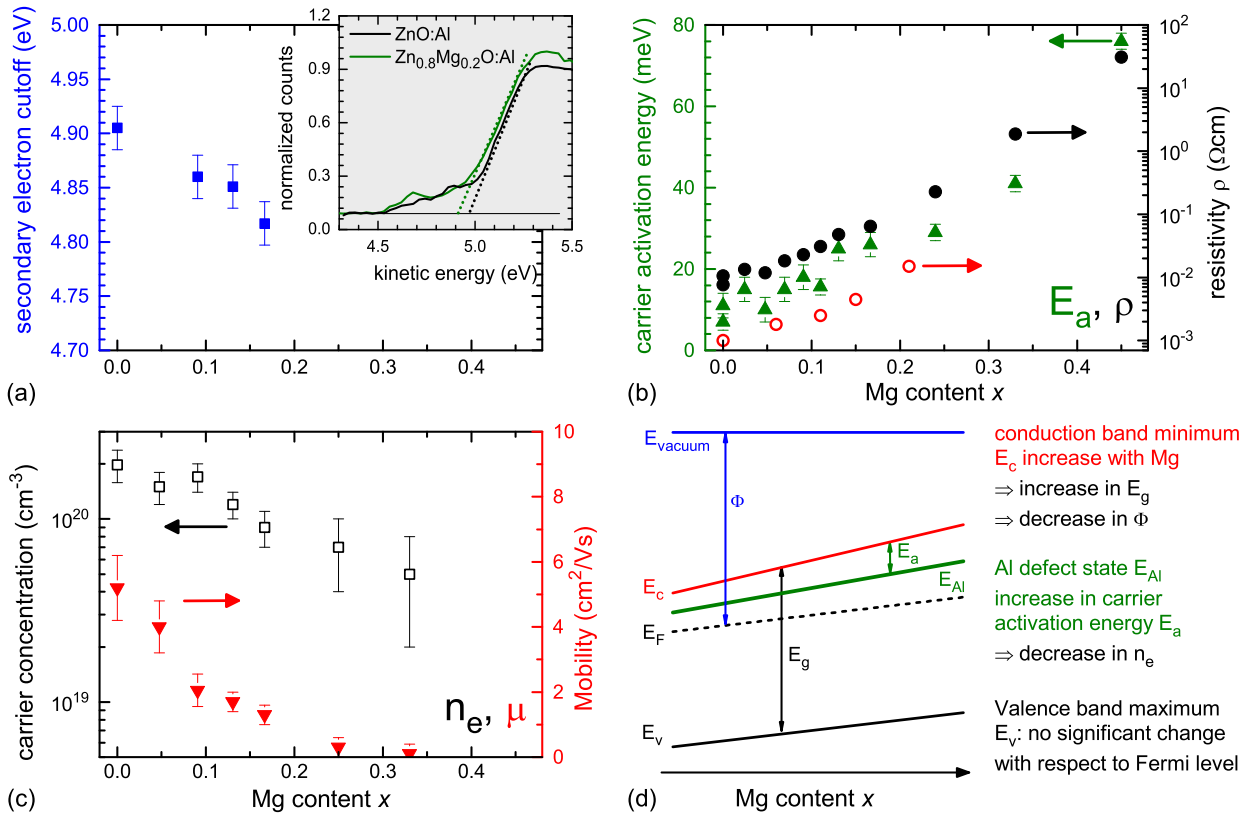

FIG. 3. Overview of the main electrical properties of $Zn_{1-x}Mg_xO$:Al as a function of Mg content. a) The reduction in the work function as measured by the secondary electron cut off in UPS measurements (■) b) The measured change in resistivity ρ (•) and effective carrier activation energy (▲). As reference resistivities of CVD grown material[13] is shown as well (○). c) Mobility (▼) and carrier concentration (□) for selected samples. d) Schematic summary of changes in the band structure consistent with all the measurements presented.

for the temperature dependent resistivity measurements from 300-450 K can explain the observed changes. This indicates, that the effective electron binding energy of the dopant site – here an Al_{Zn} substitution is increasing as a function of the Mg concentration. This then directly leads to a smaller number of activated carriers at room temperature and hence a lower number of free carriers. In order to more effectively dope the ternary $Zn_{1-x}Mg_xO$, defects other than the Al substitution have to be introduced. In particular defect complexes such as Al_{Zn}-N_O, might be able to reduce the donor binding energy. More thorough investigations or *ab-initio* calculations on the defect energies of such ternary materials would be required.

In contrast to the undoped $Zn_{1-x}Mg_xO$ system, the substantial conductivity of the doped layers makes such films potentially suitable buffer layers in OLED or solar cell devices, if a reduced refractive index *or* lower work function is required at the transparent contact. For example at a magnesium concentration of $x = 0.3$ the refractive index (n∼1.8) in the visible region (∼2.0 eV) is ideal for minimising reflective losses at glass/TCO interfaces, while still being conductive with ρ∼1Ωcm. While the resistivity of our layers is high compared to high quality ZnO:Al, this is due to the limitation in our growth technique and film thickness (300-400 nm). Spray pyrolysis is known to produce material with lower crystalline quality, many grain boundaries and hence lower electron mobilities. In addition a high number of compensating point defects due to the use of precursor chemicals with low purity reduces the achievable carrier concentration. Indeed our best case ZnO:Al reference samples only show a resistivity of $7{\cdot}10^{-3}$ Ωcm, comparable to what can be best achieved by spray pyrolysis.[18] Films grown by PLD, PECVD or magnetron sputtering show typically one order of magnitude better conductivity values.[13,15] As seen in Fig. 3b, the general trend of conductivity upon increase of Mg content is similar though. It is therefore expected that if $Zn_{1-x}Mg_xO$:Al at higher Mg concentration is grown with such techniques, the conductivity of the reduced work function, low refractive index TCO can be improved. Based on the trends found in spray pyrolysis grown samples we also expect a larger reduction in work function for samples with x>0.2, which we could

not analyse due to potential charging difficulties in UPS measurements for thin films on glass substrates. Even a small reduction in work function of 100 meV as observed here for the films with $x{\sim}0.2$ could help to improve carrier injection in devices limited by a contact resistance due to work function mismatch at the front contact.

In conclusion we have shown that the quaternary oxide $Zn_{1-x}Mg_xO$:Al can be used to tune the optical and electrical properties of this transparent conducting oxide. In particular for high magnesium content $x > 0.2$ the refractive index can be significantly lowered, making the material a good candidate for *conductive* anti-reflective coatings for Si, or at glass–TCO interfaces. In addition a reduction in work function was observed in the investigated range of magnesium content.

The authors would like to acknowledge financial support of Science Foundation Ireland under grant SFI 06/IN.1/I91 TIDA Feasibility 10.

[1] H. Hosono, Thin Solid Films **515**, 6000 (2007).
[2] W. Beyer, J. Hupkes, and H. Stiebig, Thin Solid Films **516**, 147 (2007).
[3] G. J. Exarhos, ECS Transactions, Advanced Materials and Concepts for Energy Harvesting **19**, 29 (2009).
[4] H. Liu, V. Avrutin, N. Izyumskaya, U. Ozgr, and H. Morkoc, Superlattices and Microstructures **48**, 458 (2010).
[5] K. Fleischer, E. Arca, and I. V. Shvets, Sol. Energ. Mat. Sol. Cells **101**, 262 (2012).
[6] T. Minemoto, T. Negami, S. Nishiwaki, H. Takakura, and Y. Hamakawa, Thin Solid Films **372**, 173 (2000).
[7] R. Schmidt, B. Rheinlander, M. Schubert, D. Spemann, T. Butz, J. Lenzner, E. M. Kaidashev, M. Lorenz, A. Rahm, H. C. Semmelhack, and M. Grundmann, Appl. Phys. Lett. **82**, 2260 (2003).
[8] T. Takagi, H. Tanaka, S. Fujita, and S. Fujita, Jpn. J. Appl. Phys. **42**, L401 (2003).
[9] X. Dong, B. L. Zhang, X. P. Li, W. Zhao, R. S. Shen, Y. T. Zhang, X. C. Xia, and G. T. Du, Semicond. Sci. Technol. **23** (2008).
[10] Y. S. Choi, J. W. Kang, D. K. Hwang, and S. J. Park, IEEE Trans. Electron Devices **57**, 26 (2010).
[11] K. Koike, K. Hama, I. Nakashima, S. Sasa, M. Inoue, and M. Yano, Jpn J Appl Phys 1 **44**, 3822 (2005).
[12] T. Torndahl, C. Platzer-Bjorkman, J. Kessler, and M. Edoff, Prog. Photovoltaics **15**, 225 (2007).
[13] J. G. Lu, S. Fujita, T. Kawaharamura, H. Nishinaka, Y. Kamada, and T. Ohshima, Appl. Phys. Lett. **89** (2006).
[14] R. K. Gupta, K. Ghosh, R. Patel, and P. K. Kahol, Mater Sci Eng B-Adv **156**, 1 (2009).
[15] K. Matsubara, H. Tampo, H. Shibata, A. Yamada, P. Fons, K. Iwata, and S. Niki, Appl. Phys. Lett. **85**, 1374 (2004).
[16] P. Lautenschlager, M. Garriga, L. Vina, and M. Cardona, Phys. Rev. B **36**, 4821 (1987).
[17] X. Jiang, F. L. Wong, M. K. Fung, and S. T. Lee, Appl. Phys. Lett. **83**, 1875 (2003).
[18] A. Crossay, S. Buecheler, L. Kranz, J. Perrenoud, C. M. Fella, Y. E. Romanyuk, and A. N. Tiwari, Sol. Energ. Mat. Sol. Cells **101**, 283 (2012).